*Fountain Journal of Basic Medical and Health Sciences (FUJBMHES), 1*(2), 56-76.

# Dye Degradation from Aqueous Solution by Green Synthesised Silver Nanoparticles (AgNPs) from Smooth Pigweed (*Amaranthus hybridus*): Kinetics and Thermodynamics Studies

**Bamigbade, A.A.[1*], Oduntan, K. D. [1], Sulaiman, T. R.[1], Ayeni, I.[1], & Akiode, K. O.[2]**

*[1]Department of Chemistry, College of Physical Sciences, Federal University of Agriculture, Abeokuta, Nigeria;*
*[2]Department of Chemistry, Nigeria Army University, Biu, PMB 1500, Borno State, Nigeria*

**Correspondence author: akeemadesina1983@gmail.com, bamigbadeaa@funaab.edu.ng,*
*+23470 3617 8875*

## Abstract

**Background:** The **t**extile industry, predominantly the dye industry, represents the world's major contributor to water pollution. The waste from such industries makes the water bodies coloured, detrimental to terrestrial and aquatic environments. **Objectives:** This study investigated and reported Malachite green adsorption from aqueous solution using silver nanoparticles (AgNPs). **Methodology:** AgNPs were prepared via an eco-friendly approach and characterised by Fourier transform Infrared spectroscopy (FTIR), X-ray diffractometry (XRD), UV-visible spectrophotometer and Scanning electron microscopy (SEM). Adsorption study was investigated under different conditions such as, pH, adsorbent dosage, contact time, temperature and initial concentration of dye to determine the optimal conditions and the maximum adsorption capacities. **Results:** XRD revealed the crystalline nature of the AgNP. However, the SEM micrograph of the AgNPs showed a spherical shape with a non-uniform granular shape attributed to the bio-mediated process. Whereas, FTIR spectra of AgNPs exhibited 3407, 2956, 2834, 2725, 1660, 1358 and 1096 $cm^{-1}$, representing free OH molecules, stretching C-H modes, stretching alkenes C=O bonds, carbonyl group stretching C-OH band, stretching C-O alcohols and ethers, respectively. The kinetic study of malachite green onto silver nanoparticle adsorbents showed that the adsorption kinetics followed both the pseudo-first-order and pseudo-second-order rate. **Conclusion:** The AgNPs can be effective adsorbents for removing dyes from aqueous solutions. **Recommendation:** The study suggests implementing eco-friendly practices in the textile dyeing process to reduce water pollution, targeting the adoption of biodegradable materials and sustainable dyes. It further suggests conducting further research on optimising adsorption conditions using silver nanoparticles to improve pollutant removal efficiency from wastewater in the textile industry.

**Keywords:** Malachite green**;** Characterization; Adsorption; Kinetics; Silver nitrate

## Introduction

Nanoparticles are tiny particles that are between 1 and 100 nanometres in size (Wang et al., 2012). They are so small that they are invisible to the naked eye. However, they are potentially helpful for human well-being in a wide range of applications and various fields such as medicine, electronics, optics, catalysis, and materials science (Annamalai & Nallamuthu, 2016). The unique properties of nanoparticles, such as their high surface area to volume ratio, controlled size, shape, and disparity, make them attractive to various applications (Liu et al., 2013). Among all nanoparticles, noble metal nanoparticles have enormous applications in diverse areas like bio-imaging, sensors, diagnosis, and novel therapeutics in the biomedical field (Magalh et al., 2017). Metal materials in nanomaterial size, also known as metal nanomaterials, are currently widely used as research objects for several advantages compared to their bulk size, such as unique

 ISSN (online): 1595-1693

optical properties, physical properties and chemical reactivity (Gangadharan et al., 2010). Some applications of metal nanomaterials include colourimetric sensors for various analytes (Badi'ah et al., 2019; Shrivastava et al., 2022), conductors (Matsuhisa et al., 2008), anti-microbial and anti-bacterial (Ahmed et al., 2020; Li et al., 2021), and energy conversion (Annamalai & Nallamuthu, 2016). One of the widely used metal nanomaterials is silver nanoparticles.

Silver nanoparticles have an interesting morphology, size, and different maximum thermal conductivity compared to other metals (Prakash et al., 2014). In addition, silver nanoparticles have a good compound reactivity with relatively good abundance, essential physical properties and a lower price than other types of metals (Merkoci et al., 2012). Therefore, silver nanoparticles are more widely used in various applications. Recently, silver nanoparticles have been applied as antimicrobial agents in various products such as cosmetics (Khodadadi et al., 2017), animal feed (Huang et al., 2007), coating of catheters (Rusnaenah et al., 2009), wound dressing (Dung et al., 2017), and water purification (Grégorio & Pierre-Marie, 2007) with a minimal risk of toxicity in humans.

Some methods have been developed to synthesise silver nanoparticles, such as chemical reduction (Song et al., 2020), using Ketapang leaf extract (Ruan et al., 2017), Syzygium polyanthum extract (Huixuan et al., 2007) and Mangosteen bark extract (Zahoor et al., 2021). Silver nanoparticles by chemical reduction can use $NaBH_4$ as a reducing agent (Ullah et al., 2020). However, silver nanoparticles have a low stability and easily aggregate, forming flocks of a large size. Therefore, the other materials as a capping agent of silver nanoparticles are needed to prevent the aggregation between the surfaces of silver nanoparticles (Wang et al., 2013). Stabilisation of silver nanoparticles with a polymer can improve the stability, electro-optical properties, and biological applications. Polymers can bind to the surface of metal nanoparticles with several interactions, such as chemical adsorption, electrostatic interactions, and hydrophobic interactions (Punnoose & Mathew, 2018). Polymers that can be used as stabilisers for silver nanoparticles include poly-(propyleneimine) dendrimer (PPI), (Wang et al., 2012) poly- (vinylpyrrolidone) (PVP) (Pradeep, 2009), and hyperbranced polyethylenimine (PEI) (Liu et al., 2013). *Amaranthus hybridus*, also known as smooth pigweed or slim amaranth (tètè àbáláyé in Southwestern Nigerian Yoruba Language), is an annual plant in the *Amaranthaceae* family. It is a common weed found in many parts of the world, including Africa, Asia, and North America. *Amaranthus hybridus* was used in this study as a capping agent for silver nanoparticles. *Amaranthus hybridus* can be helpful in synthesising silver nanoparticles because it contains compounds that can act as reducing agents and reduce silver ions to silver nanoparticles.

Malachite green (MG) (4-[(4-dimethylaminophenyl)phenylmethyl]-N, N-dimethylaniline) is an organic compound that has numerous industrial applications, such as dyeing of silk, leather, plastics, and paper. Their appearance harms humans and animals following inhalation and/or ingestion, producing toxicity to the respiratory system and reducing human fertility. It is highly toxic to mammalian cells, carcinogenic, and can cause skin irritation. Therefore, Malachite Green from effluent is essential to protect the environment (Papinulti et al., 2006). The MG has high resistance to light oxidising agents, while its removal based on biological treatment and chemical precipitation is inefficient (Dihom et al., 2022).

Conventional biological treatment in removing dyes from wastewater is generally ineffective, as the dyes are resistant to microorganisms.


ISSN (online): 1595-1693

Moreover, the physico-chemical treatment methods are ineffective at high effluent concentrations. It is now established that Ag is considered a promising semiconductor that is extensively involved in the removal of several toxic organic contaminants through both adsorption and photo-catalytic processes due to the stability of its chemical structure, biocompatibility, strong oxidizing power, non-toxicity and low cost of the metal precursors (Bamigbade et al., 2024).

In recent years, Nanotechnology has been extended to wastewater treatment. Due to their high surface area, AgNPs exhibit enhanced reactivity. In this study, we successfully reported the biosynthesis of silver nanoparticles using *Amaranthus hybridus* leaf extract. Synthesized silver nanoparticles were used to remove dye from aqueous solution via adsorption.

## Materials and Methods

The materials used were *Amaranthus hybridus* leaves, filter paper, and silver nitrate ($AgNO_3$) procured from Sigma Chemical and Co. Malachite green was obtained from Bektoh (Germany) and characterized by its visible spectrum, which gave a molar extinction coefficient and agreed with the literature value at $\lambda_{max}$ of 619 nm (Green, 1990). All solutions were prepared with double-distilled water, and all chemicals were used without further purification. The instruments used were an Erlenmeyer flask, a beaker, a volumetric flask, a stirring rod, an analytical balance (Acculab), a shaker, and a Magnetic Stirrer (VWR Scientific). Characterization of silver nanoparticles was done using both atomic and scanning devices, which included: XRD – X-ray Diffraction crystallography, Fourier Transform Infra-red spectrophotometer (FTIR), SEM - Scanning Electron Microscopy, and UV-Vis Spectrophotometer (Shimadzu UV-2600).

### Preparation and characterization of silver nanoparticles (AgNPs)

#### *Preparation of plant extract*

*Procedure:* A fresh leaf of a vegetable plant (Amaranthus hybridus) was harvested from a farm at Camp, Abeokuta, thoroughly cleansed to remove dirt or debris, and chopped into small pieces. These pieces were then blended. Afterwards, the water was extracted with heat and filtered using Whatman filter paper. The filtrate was collected and kept at a very low temperature (state the temperature value) to synthesize the Nanoparticles further.

#### *Biosynthesis of silver nanoparticles using Amaranthus hybridus leaf extract*

*Procedure:* A 5 mL of the Amaranthus hybridus leaf extract was added to 20 ml of 1 mm aqueous $AgNO_3$ solution. The resulting solution was heated to about 70 °C. A colour change in the solution mixture from green to dark brown was observed, signifying the reaction's completion and subsequent formation of silver nanoparticles. The solution was filtered after observing the colour change, and the AgNPs were left as residue.

#### *Adsorption studies*

Adsorption studies were carried out following a procedure previously reported by Bamgbose et al. (2012). A stock solution (100 mg/ L) of Malachite green dye was prepared by dissolving 0.1 g of the dye in 1000 mL of water, and 50 mg/ L of the dye was prepared from the stock solution. Silver nanoparticle adsorbent (0.02 g) was then separately added to the prepared solutions, and the mixtures were shaken for two hours. Absorbance readings were taken using the UV-Visible spectrophotometer (Shimada UV spectrophotometer, UV- 1800) at a $\lambda_{max}$ of 420 nm. The effect of concentration, temperature, time, pH, and adsorbent dosage on adsorption was also determined. Absorbance before and after the adsorption process was taken to determine the quantity ($q_e$) of Malachite green (mg/g) dye adsorbed at equilibrium using the formula:


ISSN (online): 1595-1693

$$q_e = \left( \frac{C_o - C_e}{m} \right) \times v \quad (1)$$

where $C_o$ and $C_e$ (mg/L) are the initial and final concentrations of the adsorbates, respectively, v is the volume of the solution used (mL), and m is the mass (g) of the adsorbents. The effect of time was studied at time intervals of 10 and 90 minutes, while the effect of temperature was studied at a temperature range of 10 and 40 °C. The effect of pH was studied by varying the pH between 2 and 13 using 0.1 M HCl or 0.1 M NaOH, while the effect of concentration was studied using 50 and 250 mg/L of the adsorbate.

***Characterization of silver nanoparticles (AgNPs)***

The brown coloured silver nanoparticle solution, which arises due to excitation of surface Plasmon vibrations of the silver nanoparticles, was subjected to UV-Visible spectra recording using a Shimadzu UV-1601 double-beam spectrometer with quartz cuvettes of 1cm path length. The UV-Visible spectrum of AgNP was presented in Fig.1. The Surface Plasmon Resonance (SPR) peak of AgNP, equivalent to the maximum absorbance peak, occurs at 420nm. The AgNPs with a 7-10 nm size range mostly showed the SPR peaks at 420nm (Modrzejewska et al., 2010). The overall observations suggested that the bio-reduction of silver ions ($Ag^+$ to $Ag^0$ was confirmed by UV-Visible spectroscopy.

The FTIR spectra were recorded in KBr pellets for AgNP at 25 °C using the ABBBOMEM MB 3000 Instrument. The SEM photographs of the AgNPs were measured using the Hitachi SU 6600 Instrument. The phase variety and grain size of synthesized silver nanoparticles were determined by X-ray diffraction spectroscopy (Philips PAN analytical). The synthesized nanoparticle was studied with Cu-Kα radiation at a voltage of 30 kV and a current of 20 mA with a scan rate of 0.03 °/s, λ = 1.54 Ås. The morphological features of synthesized silver nanoparticles were studied by NOVA NanoScanning Electron Microscope (JSM—6480 LV). The SEM slides were prepared by smearing the solutions on slides. A thin layer of platinum was coated to make the samples conductive. Lastly, the samples were characterized in the SEM at an accelerating voltage of 5 KV, emission current of 75 to 80 A, and working distance of 6 to 13 nm.

**Results and Discussion**

***Results of X-ray Diffraction Spectroscopy***

The XRD diffraction pattern in Fig. 2 shows that silver nanoparticles have formed. The structures of synthesized silver nanoparticles confirmed their cubic face-centred structure. The observed four sharp diffractions supported this, and intense peaks appeared at 2θ = 38.09°, 44.15°, 64.67°, and 77.54°, indexed to 111, 200, 220, and 311 Bragg's reflection (Borchert et al., 2005, Bamigbade et al., 2024), respectively, showing the crystalline structure of silver nanoparticles. The obtained data matched the JCPDS card number (65-2871). Moreover, the sharpness of the peak reveals that the particles are crystalline (Litvin et al., 2012). The crystallite size of the obtained silver nanoparticles were calculated to be 20 nm using Debye-Scherrer Equation ($D = k\lambda/ \beta\cos\theta$) with a relative deviation of 4.65%, where D is the average crystallite size of the nanoparticles, k is the geometric factor called Scherrer constant with a value of 0.9, λ is the wavelength of X-ray radiation source (0.15406 nm), θ is the Bragg's angle and β is the angular full-width at half maximum (FWHM = 0.004) of the XRD peak at the diffraction angle θ (Gnanadesigan et al., 2012; Jyoti et al., 2016). The XRD patterns (JCPDS, File No. 04–0783) and the structure of prepared silver nanoparticles were found to be face-centred cubic (FCC) crystal.


ISSN (online): 1595-1693

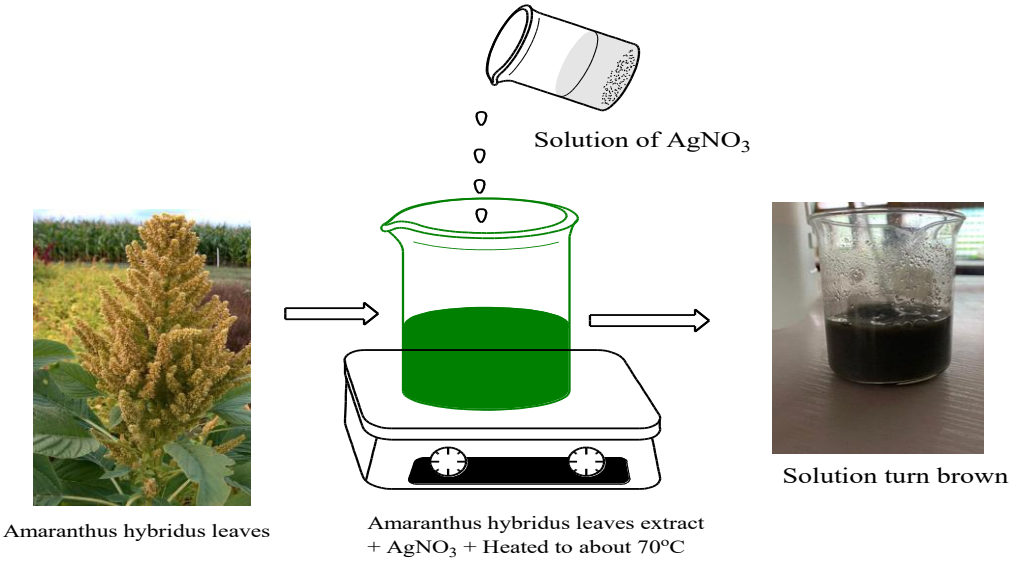


Figure 1:- Schematic representation of preparation of the Silver Nanoparticle (Bamigbade et al., 2025a).

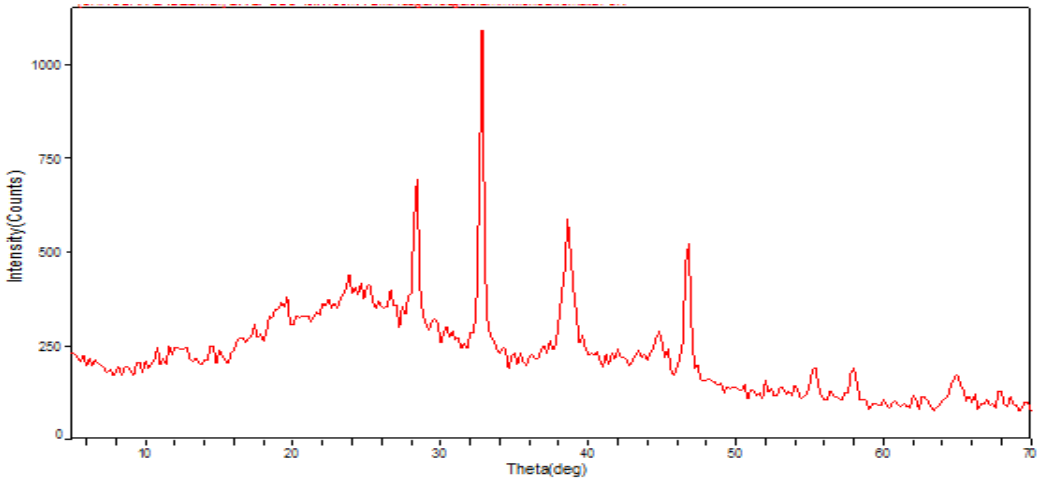


Figure 2:- XRD spectrum of Silver Nanoparticle (AgNPs)

***Results of the SEM analysis of silver nanoparticles***

The SEM analysis was carried out to determine particle morphology. Image enlargement of silver nanoparticles was performed on a scale of 80 µm with HV 5.0 Kv as presented in Fig. 3. This micrograph revealed a porous, spherical high-density structure with a non-uniform granular shape attributed to a bio-mediated process. The results of the SEM analysis further confirmed the porous nature and high surface area with attendant morphological changes in the AgNPs. The surface of the synthesized silver nanoparticles has a spherical shape and is slightly elongated, with a strong tendency to aggregate and form large particle clusters. This observation is similar to previously reported (Abdulwahid et al., 2018; Bamigbade et al., 2024, Bamigbade et al., 2025b).

***Results of UV-visible for Silver Nanoparticles***

The brown-coloured silver nanoparticle solution, which arises due to excitation of surface Plasmon vibrations of the silver nanoparticles, was subjected to UV-Visible


ISSN (online): 1595-1693

spectra recording using a Shimadzu UV-1601 double-beam spectrometer with quartz cuvettes of 1cm path length. The UV-Visible spectrum of AgNPs is presented in Fig. 4. The Surface Plasmon Resonance (SPR) peak of AgNPs, equivalent to the maximum absorbance peak, occurred at 420nm. It has been reported that AgNPs with a size range of 7-10 nm mostly show the SPR peaks at 420nm (Modrzejewska et al., 2010). The absorbance and broadening of the peak at around 420 nm indicated that the particles were monodispersed, indicating the surface plasmon resonance (SPR) absorption band due to the combined vibration of electrons in resonance with UV-visible light (Vidhu et al., 2011; Wani et al., 2010; Mallikarjun et al., 2011; Bamigbade et al., 2024, Bamigbade et al., 2025a, 2025b). The overall observations suggest that the bioreduction of silver ions ($Ag^+$ to $Ag^0$ was confirmed by UV-Visible spectroscopy.

***Results of FTIR silver nanoparticle***

The FTIR spectrum as shown in Fig. 5, Ag nanoparticles exhibit 3407, 2956, 2834, 2725, 1660, 1358 and 1096 cm-1, which represent free OH molecules, stretching C-H modes, stretching alkenes C=O bonds, carbonyl group stretching C-OH band, stretching C-O alcohols, and ethers, respectively. These peaks appeared due to the presence of flavonoids and other phenolic bio-compounds, which play a considerable role in functioning as the capping ligands, and the reduction of metal ions for synthesizing Ag-NPs. The reduced intensity and loss of bands in the wavelength after the silver nanoparticles were formed suggest that this group was responsible for the bio-reduction of silver ions. The Ag metal network was assigned 774 and 472 $cm^{-1}$ to the Ag-Ag metal NPs (Bamigbade et al., 2025a, Kemp, 1991; Wani et al., 2010; Mallikarjun et al., 2011).

**Adsorption studies**

***Effect of contact time***

The effect of contact time on the adsorption of Malachite green onto the adsorbents was studied at pH 8.0 using 50 mg/L of dye, and 0.02 g adsorbent dosage for 10 to 90 min to determine the equilibrium time for the adsorption processes. The result of the study in Fig. 6, showed that the adsorption efficiency increased gradually with an increase in contact time and reached a maximum value after 60 min for silver nanoparticles. The adsorption of the dye on the adsorbents remained constant afterwards. The increase in adsorption at the beginning of the process is primarily due to the availability of adsorption sites, which became occupied with time in the course of the adsorption process, making further adsorption onto the adsorbents insignificant (Elaigwu et al., 2014; Darwish et al., 2018, Bamigbade et al., 2024).


ISSN (online): 1595-1693

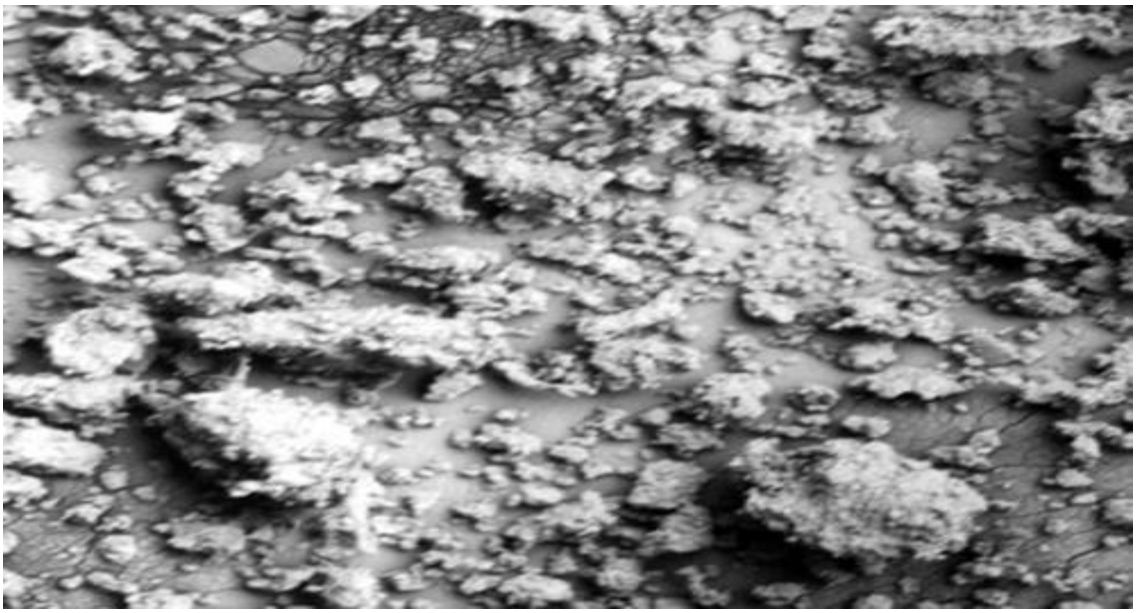

Figure 3: Scanning Electron Micrograph (SEM) of AgNPs

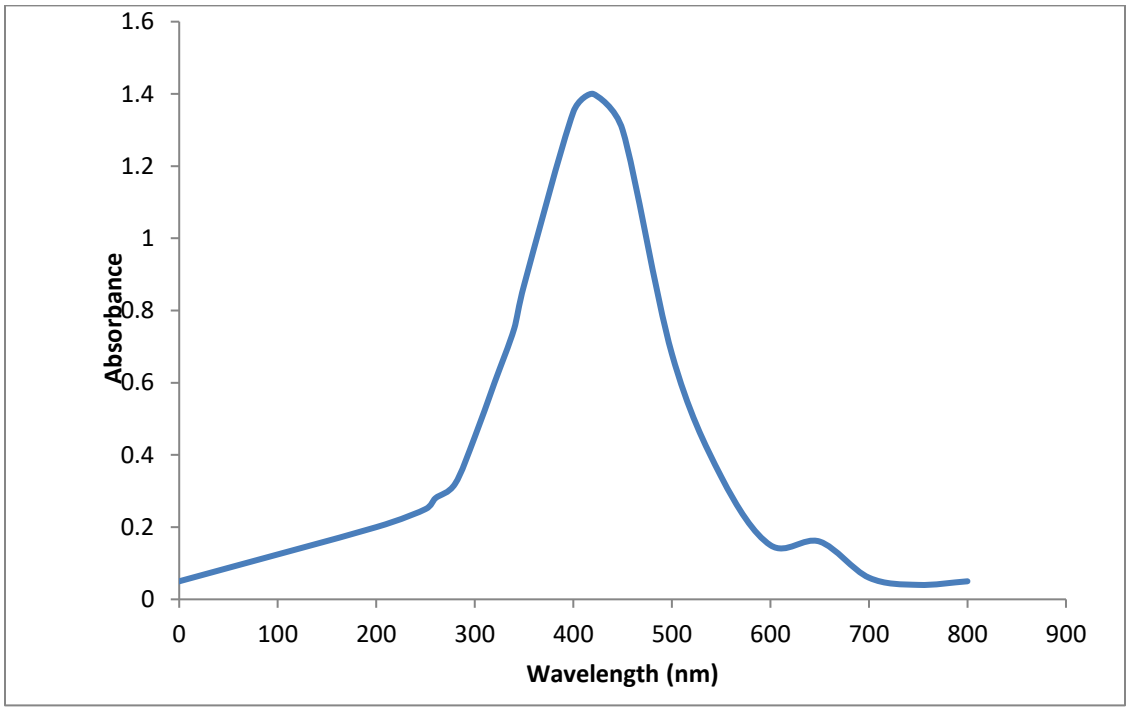


Figure 4:- UV-visible spectrum of Silver Nanoparticle (AgNPs)


ISSN (online): 1595-1693

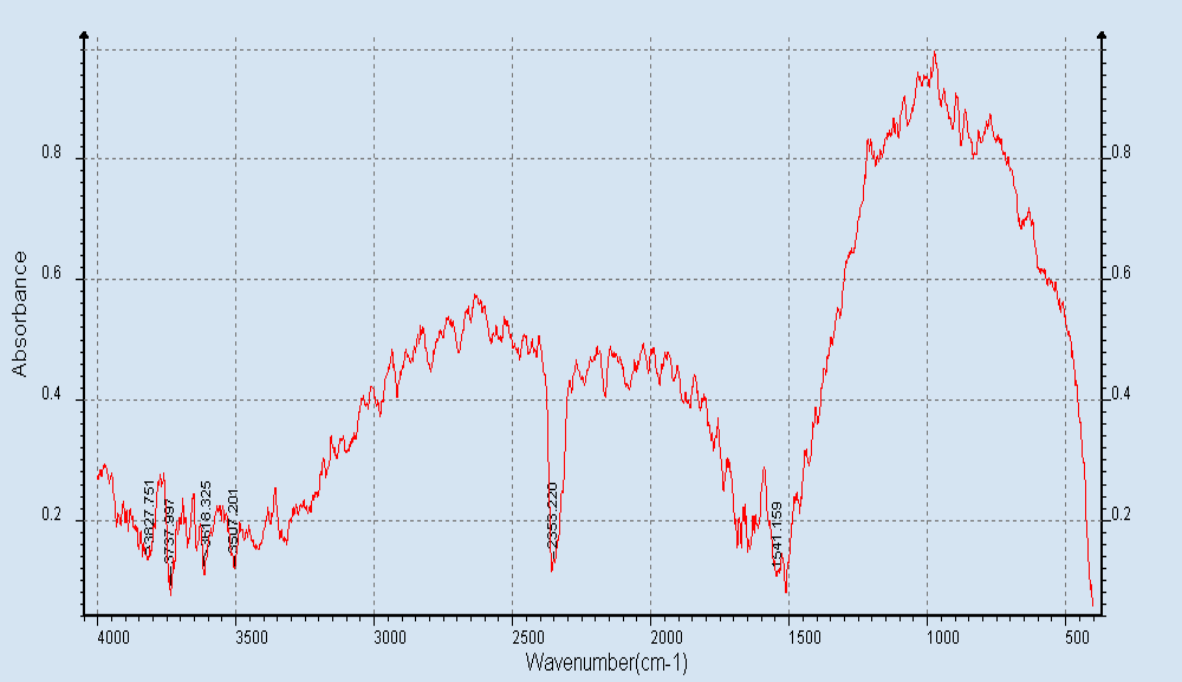


Figure 5:- FTIR spectrum of Silver Nanoparticle (AgNPs)

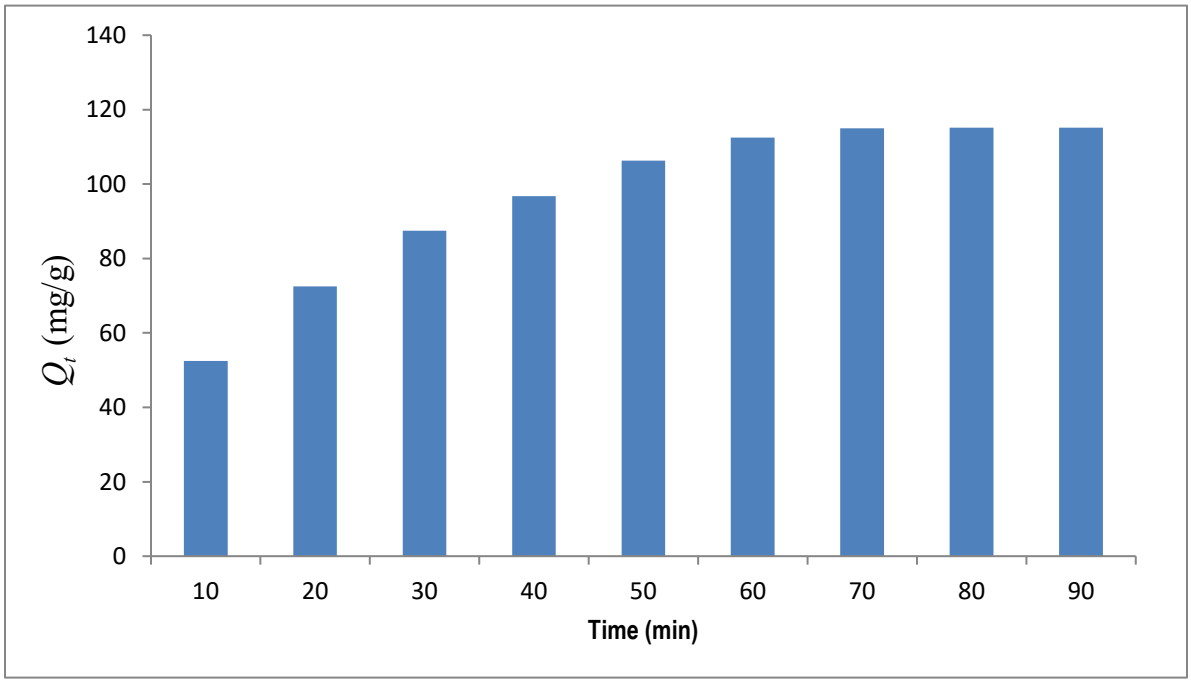


Figure 6:- Percentage Dye removed with time

***Effect of pH***

Fig. 7 shows the effect of pH on the adsorption of Malachite green onto the adsorbents. The effect was studied using the equilibrium concentrations for the adsorbents for 60 min for the experiment, while the pH was varied from 2.0 to 12.0 using 0.1 M HCl or 0.1 M NaOH. The pH affects not only the adsorption capacity but also the colour of the dye and the solubility of some dyes. Therefore, the pH value of the solution was an important controlling factor in


ISSN (online): 1595-1693

the adsorption process (Waanusantigul et al., 2003, Bamigbade et al., 2024). It can be seen from Fig. 7 that silver nanoparticles were adsorbed more at the most acidic pH value than with increasing pH value, reaching the minimum sorption process at pH 7. This led to strong dye adsorption on the acidic surface of silver nanoparticle adsorbent by an acid-base interaction mechanism between the adsorbents and the adsorbates. Thus, the adsorption mechanism can be best described by electrostatic interaction (Ilesanmi et al., 2013). However, at pH 7 the minimal sorption process observed may be a result of the interaction between the carboxylic groups of the ascorbic acid present in the capped material for the nanoparticle, and water predominates over the interaction between the adsorbent and the dye, hence the reduced adsorption (Ashok & Vikas, 2010).

Conversely, the anionic nature of Malachite green at high pH due to the presence of hydroxyl ions in its solution led to an increase in the adsorption of the dye onto the surface of the silver nanoparticle adsorbent. This can also be attributed to the binding of the Malachite green, which was first dissociated and then strongly adsorbed by silver nanoparticles through electrostatic, van der Waals, or hydrogen bonding to the adsorbent. The synergic influences of both phenomena significantly suggested a strong influence of the solution pH on Malachite green adsorption (Ilesanmi et al., 2013; Bamigbade et al., 2024). Also, when the pH of the solution was increased (above pH 7), the uptake of Malachite green increased. It appears that a change in pH solution results in the formation of different ionic species, and adsorbent surfaces. When the pH value was lower than 6, the Malachite green ions could enter the pores of the adsorbent by forming a complex on the adsorbent surface. However, at pH 7, the zwitterionic form of Malachite green in water causes the aggregation of Malachite green to form a bigger molecule (dimer). It cannot enter the pore structure of the adsorbent. At pH values higher than 8, OH-groups on the adsorbent surface enhanced the adsorption of positively charged dye cations through electrostatic forces of attraction. Hence, the increase in adsorption capacity (Arivoli et al., 2007; Bayazit et al., 2020).

### *Effect of temperature*

The effect of temperature on the adsorption of Malachite green dye onto the adsorbents was studied using the equilibrium solution concentration for each of the adsorbents. Each experiment's temperature varied from 10 to 40 ºC for 60 minutes. The study's results, shown in Fig. 8, indicated that an increase in temperature had a very minimal effect on the adsorption process. Thermodynamic parameters such as change in free energy (**Δ**G°) (kJ/mol), enthalpy (**Δ**H°) (kJ/mol) and entropy (**Δ**S°) (J/K/mol) for the adsorption processes were determined using the Van't Hoff equation:

$$\log K_o = \frac{\Delta S^o}{2.303R} - \frac{\Delta H^o}{2.303RT} \quad (2)$$

$$\Delta G^o = \Delta H^o - T\Delta S^o \quad (3)$$

$$K_o = \frac{C_{Solid}}{C_{liquid}} \quad (4)$$


ISSN (online): 1595-1693

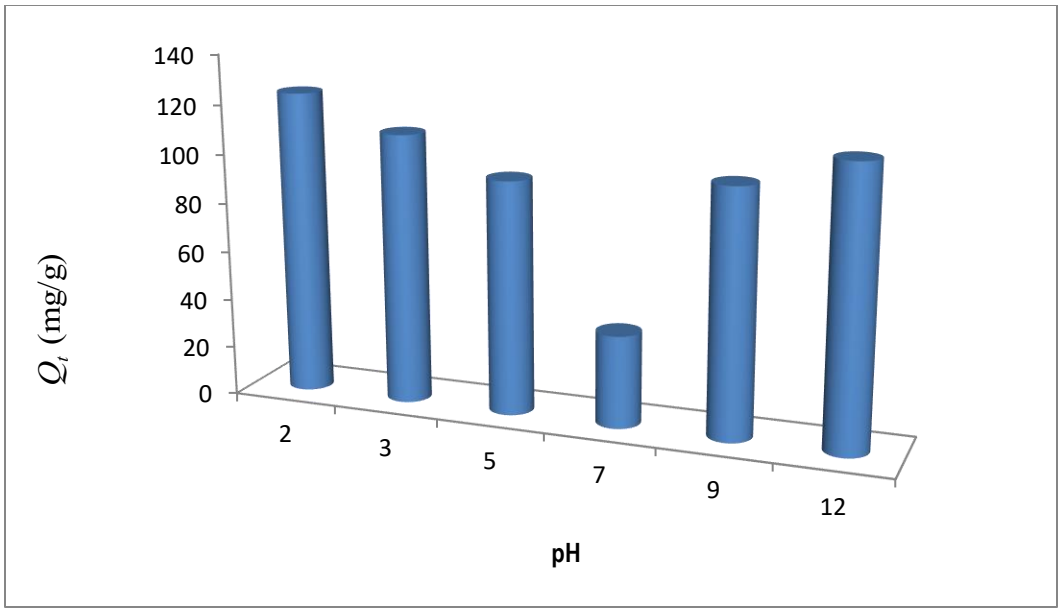


Figure 7:- Percentage Dye removed with pH

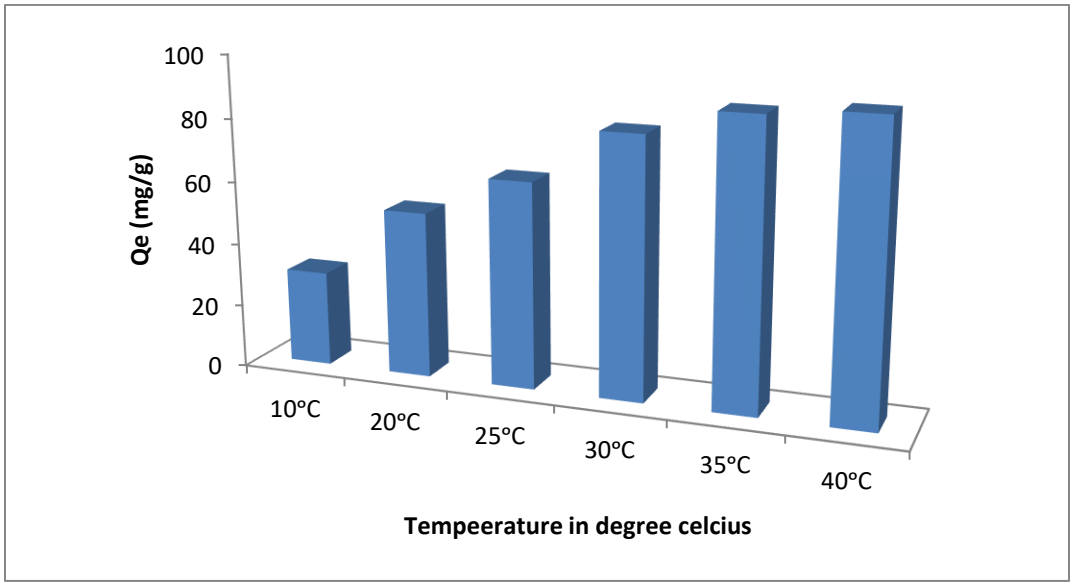


Figure 8:- Percentage Dye removed with temperature

ΔH° (kJ/mol), and ΔS° (J/mol $K^{-1}$) were evaluated from the slope and intercept of Van't Hoff plots of Equation (2) and the results obtained were 5.7741 $kJmol^{-1}$ and 39.25 $JK^{-1}mol^{-1}$, respectively. The positive values of ΔH showed the adsorption's endothermic nature, signifying the adsorption process's physisorption. The positive values of ΔS° showed that the adsorption process is entropy-driven, showing an increased disorder and randomness at the solid-solution interface of the adsorbent. The adsorbed water molecules, which are displaced by the adsorbate (dye) species, gain more translational entropy than they lose by the adsorbate molecules, thus allowing the prevalence of randomness in the


ISSN (online): 1595-1693

system (Namasivayam & Yamuna, 1995; Namasivayam et al., 1997). The value of ΔG° obtained at 25 °C, representing the prevailing room temperature, is -5.923 kJ $mol^{-1}$. The negative values of ΔG° indicated that the adsorption was highly favourable and spontaneous. From the results, we could conclude that physisorption is more efficient.

### *Adsorption kinetic studies*

The adsorption process's nature depended on the adsorbent system's physical or chemical characteristics and the system conditions. Kinetic models such as pseudo-first- and second-order, Elovich and intra-particle diffusion were used to study the rate and mechanism of the adsorption process, and the results are presented in Table 1. The pseudo-first-order (Lagergren) model was obtained by plotting the values of $\ln(q_e - q_t)$ versus *t*, and the values of $k_1$ and $q_e$ were determined from the slope and intercept of the graph, respectively (Fig. 9a).

The similarity between the intercept and the experimental $q_e$ value indicated that this model explained the experimental data, and the adsorption rate follows this equation (Lagergren, 1898; Ho, 2006). The validity of the model was further checked by the correlation coefficient ($R^2$). The high $R^2$ values again showed that the pseudo-first-order model fitted well with the experimental data.

The plot of $\frac{t}{q_t}$ versus *t* for the pseudo-second-order kinetic model presented in Fig. 9b, gave a straight line with a high correlation coefficient ($R^2$). The $k_2$ and equilibrium adsorption capacity ($q_e$) were calculated from the intercept and slope of this line, respectively. The high values of $R^2$ (0.9946) and closeness of experimental and theoretical adsorption capacity ($q_e$) value showed the pseudo-second-order model's applicability in explaining and interpreting the experimental data (Ruthven & Loughlin, 1971). The Elovich equation is another rate equation based on the adsorption capacity in linear form, which had been successfully applied for the adsorption of solutes from a liquid solution (Ruthven & Loughlin, 1971; Ho & McKay, 1999). The plot of $q_t$ versus ln (*t*) should yield a linear relationship (Fig. 10a) with a slope (1/*b*) and an intercept $\left(\frac{1}{b}\right)\ln(ab)$.

Table 2 reports the Elovich constants obtained from the slope and intercept of the straight line. The correlation coefficients ($R^2$) were high, showing that this model was completely suitable for evaluating adsorption processes (Bulut & Ozacar, 2008). The intra-particle diffusion model based on diffusive mass transfer, in which the adsorption rate can be expressed in terms of the square root of time (t) (Chien & Clayton, 1980; Ozdes et al., 2011; Ghaedi et al., 2012), was also applied. The values of $K_{diff}$ [the intra-particle diffusion rate constant ($mg/g/min^{1/2}$)] and C (thickness of the boundary layer) were calculated from the slope and intercept of the plot of $q_t$ versus $t^{\frac{1}{2}}$ presented in Fig. 10b, and the results are presented in Table 1. From the results in Table 1, it was evident that the adsorption of the dye followed both the pseudo-first- and the pseudo-second-order kinetics. The theoretical values obtained were close to experimental values with correlation coefficients >0.99, which fit better than the other kinetic models for the adsorption process. Therefore, it can be concluded that the pseudo-second-order equation is better in describing the adsorption kinetics of Malachite green on silver nanoparticle adsorbent, and therefore, the rate of reaction appeared to be controlled by the chemical interaction (Rajabi et al., 2016; Tella et al., 2019).

 ISSN (online): 1595-1693

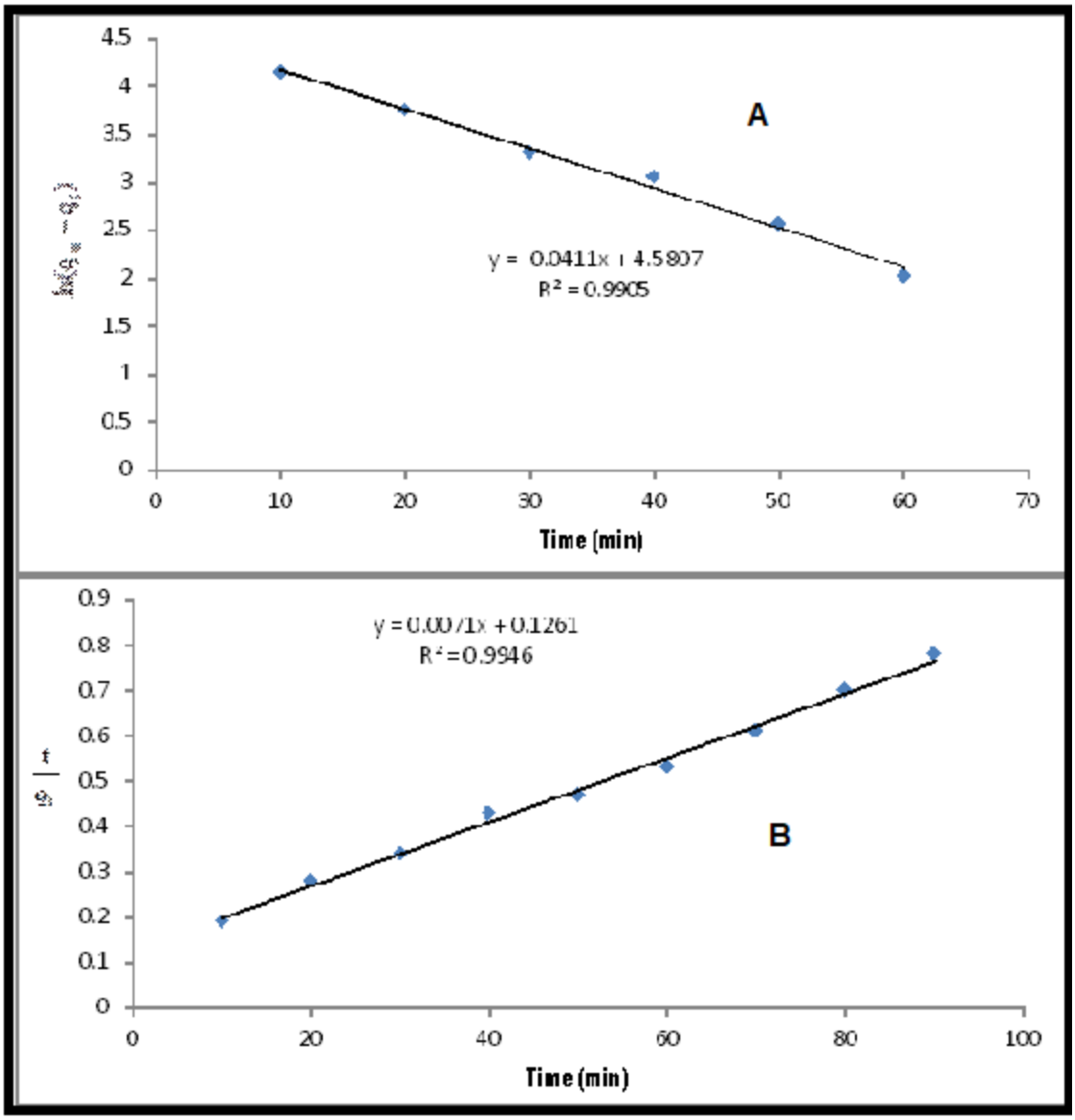


**Figure 9:-** (a) Plot of $\ln(q_e - q_t)$ versus time (min), (b) Plot of $\frac{t}{q_t}$ versus time (min)


ISSN (online): 1595-1693

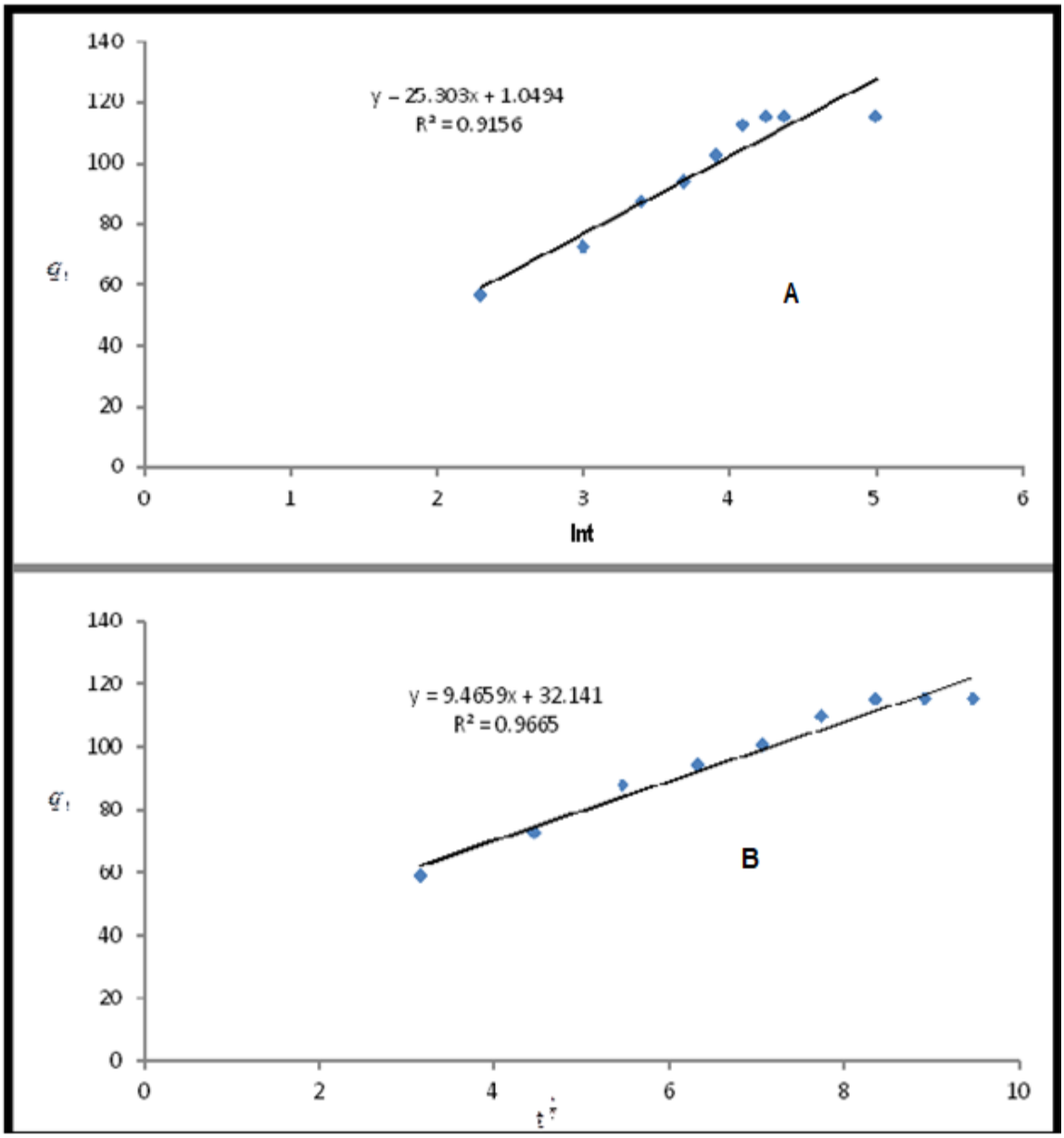


**Figure 10:-** (a) Plot of $q_t$ versus lnt, (b) Plot of $q_t$ versus $t^{\frac{1}{2}}$ (min)


ISSN (online): 1595-1693

**Table 1. Kinetic parameters of Malachite green adsorption onto silver nanoparticle**

| Models | Equations | Parameters | Adsorbents |
|---|---|---|---|
| | | | Silver nanoparticle |
| First-order kinetic model | $\ln(q_e - q_t) = \ln(q_e) - k_1 t$ | $k_1$ | 0.041 |
| | | $q_e$ (cal) | 97.58 |
| | | $R^2$ | 0.9905 |
| Second-order kinetic model | $\frac{t}{q_t} = \frac{1}{k_2 q_e^2} + \left(\frac{1}{q_e}\right) t$ | $q_e$ (cal) | 108.85 |
| | | $R^2$ | 0.9946 |
| | | $k_2$ | 0.0039 |
| Intra-particle diffusion | $q_t = K_{diff} t^{\frac{1}{2}} + C$ | C | 32.141 |
| | | $K_{diff}$ | 9.466 |
| | | $R^2$ | 0.9665 |
| Elovich | $q_t = \frac{1}{\beta}\ln(\alpha\beta) + \frac{1}{\beta}\ln(t)$ | $B$ | 0.0395 |
| | | $R^2$ | 0.9156 |
| Experimental Adsorption Capacity | | ($q_e$) | 87.96 |


ISSN (online): 1595-1693

## *Conclusion*

Silver nanoparticle was prepared via bio-reduction process and characterized by X-ray diffractometry (XRD), Scanning electron microscopy (SEM), Fourier Transform Infra-red spectroscopy (FTIR), and UV-visible spectrophotometer (UV-vis).

The crystalline size of the AgNP was revealed with XRD. The cubic face-centred structure of the synthesized silver nanoparticle was confirmed; this was supported by the observed sharp four diffraction peaks that appeared at 2θ = 38.09°, 44.15°, 64.67°, and 77.54°. However, the SEM micrograph of the synthesized AgNP revealed the spherical shape of AgNP with a non-uniform granular shape attributed to the bio-mediated ionic gelation process. The surface of the synthesized AgNP has a spherical shape and is slightly elongated with a strong tendency to aggregate and form larger particle clusters. Whereas, FTIR spectra of AgNP gave peaks that revealed the presence of flavonoids and other phenolic bio-compounds, which play a considerable role in functioning as the capping ligands, and reduction of metal ions for the synthesis of Ag-NPs. The synthesized silver nanoparticles were used as adsorbents to remove malachite green from aqueous solution

The results showed that the prepared silver nanoparticles had high adsorption capacity for malachite green. The process of adsorption was fast and attained equilibrium within 60 min. From the UV-vis indication, the AgNPs sized between 7-10 nm typically exhibit SPR peaks at 420 nm.

The silver nanoparticle was the most effective in removing malachite green due to the acid-base interaction between the adsorbent and the adsorbate as the malachite green solution is in the acidic medium. The effective pH for the study was around 4.6 for the nanoparticle adsorbents, while the optimum adsorbent dose was 0.02 g. The kinetic study of malachite green onto silver nanoparticle adsorbents showed that the adsorption kinetics followed both the pseudo-first-order and pseudo-second-order rate. The results from this study indicate that silver nanoparticles obtained using a simple method like the one adopted in this research could be utilized as effective adsorbents for removing dyes from wastewater.

**Recommendations:**

- *Optimize Synthesis Conditions:* Further investigate the effect of different synthesis parameters such as temperature, reaction time, and precursor concentration on the size and stability of the silver nanoparticles;
- *Expand Characterisation Techniques:* Use additional techniques, such as Transmission Electron Microscopy (TEM) and Scanning Electron Microscopy (SEM), to provide more comprehensive insights into the morphology of the nanoparticles.
- *Explore Functional Applications:* Assess the antibacterial and catalytic properties of the synthesised silver nanoparticles to determine their potential industrial and medical applications.
- *Conduct Long-term Stability Tests:* Evaluate the stability and reactivity of the silver nanoparticles over extended periods to ascertain their longevity in practical applications.
- *Investigate Toxicity:* Perform toxicity studies on biological systems to establish the safety of silver nanoparticles for medical or agricultural use.
- *Comparative Studies:* Conduct comparative studies with silver nanoparticles synthesised via different methods to benchmark the crystallinity and size distributions.
- *Scale-up Production:* Explore scalable methodologies for producing silver nanoparticles to facilitate commercial applications while maintaining quality control.

**Limitations to the study:**

- *Narrow Focus on Synthesis Parameters:* The study investigates specific fabrication methods without considering alternative synthesis routes that may yield better results.
- *Limited Characterisation Techniques:* Only X-ray Diffraction (XRD) was employed for crystallinity assessment, which may not capture all structural characteristics of the nanoparticles.


ISSN (online): 1595-1693

- *Lack of Biological Context:* The study does not explore the interaction of silver nanoparticles with biological systems or their ecological impact, limiting applicability in biomedical fields.
- *Potential Measurement Errors:* Possible inaccuracies in measuring peak intensities and positions in XRD could affect the reliability of the derived crystallite sizes.
- *Static Analysis:* The analysis is based on a singular measurement without dynamic assessments of particle behaviour under varying environmental conditions.
- *Sample Size:* The sample size may not be representative enough to generalize the findings across different formulations of silver nanoparticles.
- *Limited Temporal Perspective:* The study's findings are based on a snapshot in time, which may not reflect changes that occur with prolonged environmental exposure or use.

**Scientific Implications:**

- *Advancement of Nanotechnology:* The successful synthesis and characterisation of silver nanoparticles contribute to the growing field of nanotechnology and its varied applications.
- *Foundation for Future Research:* This study provides a baseline for future research focused on functionalizing silver nanoparticles for targeted applications, paving the way for innovations in medicine and catalysis.
- *Insight into Crystalline Structures:* The detailed analysis of crystalline structures enhances understanding of the properties influencing nanoparticle behaviour, which is critical for their application.
- *Potential for Industrial Adoption:* The findings support potential scalability for industrial production, which is vital for commercialising silver nanoparticles in various sectors.
- *Environmental Considerations:* Understanding the synthesis and properties of nanoparticles will aid in risk assessments regarding their environmental and health impacts.
- *Contribution to Material Science:* This research enhances material science knowledge, especially in developing materials with tailored properties that benefit various technological advancements.
- *Stimulating Interdisciplinary Research:* The implications of silver nanoparticles may inspire interdisciplinary studies combining chemistry, biology, and materials science to solve complex challenges.

## Ethical consideration:

The authors declare no ethical issues

## Conflict of interest:

The authors declare no conflict of interest

## Acknowledgements

The authors wish to thank the Chemistry Department of Covenant University, Ota, staff for their assistance in running the scanning electron micrograph of the nanoparticles. All other nanoparticle characterization was carried out at the Chemistry Department, FUNAAB. The work was carried out in the postgraduate research laboratories of the Department of Chemistry, FUNAAB. We are grateful to the Management of Federal University of Agriculture, Abeokuta (FUNAAB), for supporting the equipment used in this research.

## References

Abdulwahid, W., Abdul, K., Nursiahla, N.N., & Wayan, S. (2018). Synthesis of Silver Nanoparticles using Muntingia calabura L. Extract as Bioreductor and Applied as Glucose Nanosensor. *CODEN: OJCHEG,* 34(6), 3088-3094.

Ahmed, T., Noman, M., Shahid, M., Niazi, M.B.K., Hussain, S., & Manzoor, N. (2020). Green synthesis of silver nanoparticles transformed synthetic textile dye into less toxic intermediate molecules through LC-MS analysis and treated the actual wastewater. *Environ Res.,* 191, 110-142. https://doi.org/10.1016/j.envres2020.110142.

Arivoli, S., Sudha, R., Kalpana, K., & Rajachandrasekar, S. (2007). Comparative study on Adsorption kinetics and Thermodynamics of Metal ions onto Acid

 ISSN (online): 1595-1693

Activated Low-Cost Pandanus Carbon. *E. Journal of Chemistry,* 4(2), 238-254.

Ashok, K.T., & Vikas, R. (2010). Cross-linked Chitosan films: Effect of cross-linking Density on Swelling parameters. *PaTk. J. Pharm. Sci.,* 23(4), 443-448.

Badi'ah, S., Supriya, T.O., & Mahltig, Z.B. (2019). Microwave-assisted synthesis of silver nanoparticles: effect of reaction temperature and precursor concentration on fluorescent property. *J. Clust Sci.,* 33, 101–111. https:// doi. org/10.1007/s10876-020-01945-x.

Bamgbose, J.T., Bamigbade, A.A., Nkiko, M.O., Ahmed, S.A., & Ikotun, A.A. (2012). Kinetics and thermodynamic studies of adsorption of malachite green onto unmodified and EDTA-modified groundnut husk. *African Journal of Pure and Applied Chemistry,* 6(14), 141–152.

Bamigbade A.A., Oduntan K.D. and Bamgbose J.T. (2024). Chitosan Assisted Silver Nanoparticles for Degradation of Dyes from Aqueous Solution: Kinetic and Thermodynamic Studies. *Journal of Chemical Society of Nigeria*, 49(3), 444-469.

Bamigbade, A.A., Oduntan, K.D., Sulaiman, T.R., Ayeni, I. and Akiode K.O. (2025a). Synthesis and application of Silver Nanoparticles (AgNPs) Adsorbent produced from *AmaranthuS hybridus* for the removal of Malachite green dye. *Proceedings of the Nigeria Academy of Science*. 18(1), 79-98.

Bamigbade, A.A., Oduntan, K.D., Sulaiman, T.R., Ayeni, I., Akiode K.O., Mohamed, H., Ali El G., Talha Bin E. and Ofudje, A.E. (2025b): Malachite Green adsorption from Aqueous Medium by Chitosan Assisted Silver Nanoparticles (AgNPs): Isotherm and Thermodynamics Studies. *Bull. Chem. Soc. Ethiop.*, 39(7), 1283-1299.

Bayazit, G., Tastan, B.E., & Gul, U.D. (2020). Biosorption, Isotherm and kinetic Properties of Common Textile dye by *Phormidium animale*. *Global NEST Journal,* 22(1), 1-7.

Borchert, H., Shevchenko, E.V., Robert, A., Mekis, I., Kornowski, A., Grubel, G., & Weller, H. (2005). Silver nanoparticles: Large-scale solvothermal synthesis and optical properties. *Langmuir,* 21, 1931-1936.

Bulut, E., & Ozacar, M. (2008). Adsorption of malachite green onto bentonite: Equilibrium and kinetic studies and process design. *Microporous Mesoporous Materials*, 115*,* 234–246

Can, L., Annamalai, J., & Nallamuthu, T. (2016). Green synthesis of silver nanoparticles: characterisation and determination of antibacterial potency. *Applied Nanosci.,* 6(2):259-265.

Chien, S.H., & Clayton, W.R. (1980). Application of the Elovich equation to the kinetics of phosphate release and sorption on soil. American Journal of Soil Science Society 44*,* 265–268

Darwish, A.A.A., Rashad, M., & Al-aoh, H.A. (2018). Methyl orange adsorption comparison on nanoparticles: isotherm, kinetics, and thermodynamic studies. *Dyes Pigments,* 160, 563–571.

Dihom, H.R., Al-Shaibani, M.M., Mohamed, R.M.S.R., Al-Gheethi, A.A., Sharma, A., & Khamidun, M.H.B. (2022), Photocatalytic degradation of disperse azo dyes in textile wastewater using green zinc oxide nanoparticles synthesized in plant extract. *Water,* 15(16), 471-485

Dung, C.T., Doanh, S.C., Quynh, L.M., Hong, T.T., Quach, T.D., & Kim, D.H. (2017), Synthesis of bifunctional $Fe_3O_4$@$SiO_2$-Ag magnetic-plasmonic nanoparticles by an ultrasound assisted chemical method. *J. Electron. Mater.,* 46, 3646–3653.

 ISSN (online): 1595-1693

Elaigwu, S.E., Rocher, V., Kyriakou, G. & Greenway, G.M. (2014), Removal of $Pb^{2+}$ and $Cd^{2+}$ from aqueous solution using chars from pyrolysis and microwave-assisted hydrothermal carbonization of Prosopis africana shell.' *Journal of Industrial and Engineering Chemistry,* 205: 3467–3473.

Gangadharan, D., Harshvardan, K., Gnanasekar, G., Dixit, D., Popat, K.M., & Anand, P.S. (2010) Polymeric microspheres containing silver nanoparticles as a bactericidal agent for water disinfection. *Water Research*, 44(18):5481-5487.

Ghaedi, M., Azad, F.N., Hajati, S., Dashtain, K., Goudarzi, A., & Soylak, M. (2018). Central Composite design and genetic algorithm applied for the optimization of ultrasonic-assisted removal of malachite green by ZnO Nanorod-loaded activated carbon. *Spectrochim. Acta, Part A,* 167, 157-164

Ghaedi, M., Biyareh, M.N., Nasiri, Kokhdan, S., Shamsaldini, S., Sahraei, R., Daneshfar, A., & Hahriyar, S. (2012), Comparison of the efficiency of palladium and silver nanoparticles loaded on activated carbon and zinc oxide nano rods loaded on activated carbon as new adsorbents for removal of Congo red from aqueous solution: Kinetic and isotherm study, *Material Science and Engineering C*, 32, 725–734

Gnanadesigan, M., Anand, M., & Ravikumar, S. (2012), Antibacterial potential of biosynthesised silver nanoparticles using Avicennia marina mangrove plant. *Appl. Nanosci.,* 2, 143–147.

Green, F.Y. (1990). Sigma – Aldrich hand-book of stain dyes and indicators. Aldrich Chemical Company, Milwaukee. Pp. 224-228.

Grégorio, C., & Pierre-Marie, B. (2007), Application of chitosan, a natural aminopolysaccharide, for dye removal from aqueous solutions by adsorption processes using batch studies. *Journal of Progress in Polymer Science,* 33, 399-477.DOI: 10.1016/j.progpolymsci.2007.11.001

Ho, Y.S. (2006), Review of second-order models for adsorption systems, *Journal of Hazardous Materials*, 136, 681–689.

Ho, Y.S., & McKay, G. (1999), Pseudo-second order model for sorption processes. *Process & Biochemistry*, 34, 451–456

Huang, J., Li, Q., Sun, D., Lu, Y., Su, Y., Yang, X., & Wang, H. (2007), Biosynthesis of silver and gold nanoparticles by novel sundried Cinnamomum camphora leaf. *Nanotechnology*, 18(10), 105-118

Huixuan, W., Yuaneng, W., Wenyao, S., He, N., Hong, J., & Chen, C. (2007), Biosynthesis of silver and gold nanoparticles by novel sundried Cinnamomum camphora leaf. *Nanotechnology*. 34(8), 456-468. doi:10.1088/0957-4484/18/10/105104.

Ilesanmi, O., Oluwabamise, L.F., & Anthony, O.O. (2013). Kinetic, Equilibrium and Thermodynamic Studies of Adsorption of methylene blue from Synthetic Waste Water using Cow Hooves. *British Journal of Applied Sciences & Technology,* 3(4), 1006-1021.

Jyoti, K., Baunthiyal, M., & Singh. A. (2016). Characterization of silver nanoparticles synthesized using Urtica dioica Linn. leaves and their synergistic effects with antibiotics. *J. Radiat. Res. Appl. Sci.,* 9(3), 217–227, DOI: 10.1016/j.jrras.2015.10.002.

Kemp, W. (1991). Infrared Spectroscopy. Macmillan Press, London, pp.19-56.

Khodadadi, B., Bordbar, M., & Yeganeh-Faal, A. (2017). Green synthesis of Ag nanoparticles/clinoptilolite using Vaccinium macrocarpon fruit extract and its excellent catalytic activity for reduction of organic dyes. *Journal of Alloys Compound,* 719, 82-98.

 ISSN (online): 1595-1693

Lagergren, S. (1898). Zur theorie dersogenannten adsorption geloster stoffe kungliga svenska vetenskapsakademiens, *Handlingar,* 24*,* 1–39.

Li, Y., Sun, S., Gao, P., Zhang, M., Fan, C., Lu, Q., Li, C., Chen, C., Lin, B., & Jiang, Y. (2021). A tough chitosan-alginate porous hydrogel prepared by simple foaming method. *J. Solid State Chem.,* 294, 121-197. doi: 10.1016/j.jssc.2020.121797.

Litvin, V.A., Galagan, R.L., & Minaev, B.F. (2012), Kinetic and mechanism formation of silver nanoparticles coated by synthetic humic substances. *Colloids Surf A Physico. Chem. Eng.,* 414, 234–243.

Liu, X., Jia, F., Li, L., Mallapragada, S., Narasimhan, B., & Wang, Q. (2013). Multifunctional nanoparticles for targeted delivery of immune activating and cancer therapeutic agents. *J. Control. Release,* 172:1020–1034.

Magalh, S., Santos, L.B., Lopes, L.G., Estrela, C.R.D.A., Estrela, C., & Torres, É.M. (2017). Nanosilver application in dental cements. *ISRN Nanotechnology,* ID 365438, 6 pages.

Mallikarjun, K., Narsimha, G., Dillip, G., Praveen, B., Shreedhar, B., & Lakshmi, S. (2011), Green synthesis of silver nanoparticles using Ocimum leaf extract and their characterization. *Dig J Nanomater Biostruct.,* 6, 181–186.

Matsuhisaet, O., Deng, K.K., Kim, N., Ross Jr, L., Surampalli, R.Y., & Hu, Z. (2008). The inhibitory effects of silver nanoparticles, silver ions, and silver chloridae colloids on microbial growth. *Water Research,* 45, 3066-3074.

Merkoci, A., Asmat, U., Abad, K., & Ismail, K. (2012). Diabetes mellitus and oxidative stress-a concise review. *Saudi Pharm J.,* 24, 547–553.

Modrzejewska, Z., Zarzychi, R., & Sielski, J. (2010). Synthesis of silver nanoparticles in a chitosan solution. *Progress on Chemistry and Application of Chitin,* 15, 63-72.

Namasivayam, C., & Yamuna, R.T. (1995). Adsorption of direct red by biogas residual slurry. *Environ. Pollut.,* 89, 1-29.

Namasivayam, C., Muniasamy, N., Gayathri, K., Rani, M., & Reganathan, K. (1997). Removal of dyes from aqeous solution by cellulosic wasteorange peal. *Biores. Technol.,* 57, 37-42.

Nekouei, F., Kargarzadeh, H., Nekouei, S., Tyagi, I., Agarwal, S., & Gupta, V.K. (2019). Preparation of Nickel hydroxide nanoplates modified activated carbon foe Malachite green removal from solution: Kinetics, thermodynamics, isotherm and antibacterial studies. *Process. Saf. Environ.,* 102, 85-97.

Ozdes, D., Duran, C., & Senturk, H.B. (2011). Adsorptive removal of Cd(II) and Pb(II) ions from aqueous solutions by using Turkish illitic clay. *J of Env Man.*, 92*,* 3082–3090.

Papinulti, L., Mouso, N., & Forchiassin, F. (2006). Removal and degradation of the fungicide dye malachite green from aqueous solution using the system wheat bran – Fomessclerodermeus. *Enzy. Microb. Technol.,* 39: 848-853.

Pradeep, T. (2009). Noble metal nanoparticles for water purification: a critical review. *Thin solid films,* 517(24), 6441-6478.

Prakash, G., Ahmad, Z., Manzoor, M.Z., Mujahid, M., Faheem, Z., & Adnan, A. (2014), Optimization for biogenic microbial syn-thesis of silver nanoparticles through response surface. *Langmuir*, 27(2):720-726.

Punnoose, M.S., & Mathew, B. (2018), Treatment of Water Effluents Using Silver Nanoparticles. *Material Sci. & Eng.,* 2(5), 59-66. DOI: 10.15406/mseij.208.02.00050

 ISSN (online): 1595-1693

Rajabi, M., Mirza, B., Mahanpoor, K., Mirjalili, M., Moradi, O., Najafi, F., Sadegh, H., Shahryari-Ghoshekandi, R., Asif, M., Tygi, I., & Agarwal, S. (2016). Adsorption of Malachite green from Aqueous solution by Carboxylate group functionalized multi-walled carbon nanotubes: determination of equilibrium and kinetics parameters. *Journal of Ind. Eng. Chem.,* 34, 130-138.

Ruan, W.Q., Pan, X.D., Shen, F., & Chen, G.Q. (2017). A review of recent advances in the catalytic synthesis of polyesters and biopolyesters. *Chemical Society Reviews,* 46(16), 4819-4839. doi: 10.1039/c7cs00295a.

Rusnaenah, Z., Budi, K., Kathiravan, J., & Rajendiran, K.N. (2009). Phyllanthinassisted biosynthesis of silver and gold nanoparticles: a novel biological approach. *Journal of Nanoparticle Research.,* 11(5):1075-1085.

Ruthven, D.M., & Loughlin, K.F. (1971). The effect of crystallite shape and size distribution on diffusion measurements in molecular sieve. *Chemical Engineering Science*, 26*,* 577–584.

Shah, K.A., & Tali, B.A. (2016). Synthesis of carbon nanotubes by catalytic chemical vapour deposition: A review on carbon sources, catalysts and substrate. *Mater.Scie. Semicond. Process,* 41, 67-82

Shrivastava, V., Ali, I., Marjub, M.M., Rene, E.R., & Soto, A.M.F. (2022). Nanocomposites via in-situ co-reduction of the oxides. *Powder Technol.,* 233, 208–214.

Song, J., Han, G., Wang, Y., Jiang, X., Zhao, D., Li, M., Yang, Z., Ma, Q., Parales, R.E., & Ruan, Z. (2020). Pathway and kinetics of malachite green biodegradation by Pseudomonas veronii. *Sci. Rep.,* 10, 4502-4519. https://doi.org/10.1038/s41598-020-61442-z.

Tang, Y., Zeng, Y., Hu, T., Zhou, Q., & Peng, Y. (2016). Preparation of Lignin sulfonate-based mesoporous materials for adsorbing malachite green from Aqueous solution. *J. Environ. Chem. Eng.,* 4(3), 2900-2910.

Tella, A.C., Oladipo, A.C., Adimula, V.O., Ameen, O.A., Bourne, S.A., & Ogunlaja, A.S. (2019). Synthesis and crystal structures of a copper(II) dinuclear complex and zinc(II) coordination polymers as materials for efficient oxidative desulfurization of dibenzothiophene. *New J. Chem.,* 43, 14343—14354.

Ullah, I., Khalil, A.T., Ali, M., Iqbal, J., Ali, W., Alarifi, S., & Shinwari, Z.K. (2020), Green-Synthesized Silver Nanoparticles Induced Apoptotic Cell Death in MCF-7 Breast Cancer Cells by Generating Reactive Oxygen Species and Activating Caspase 3 and 9 Enzyme Activities. *Oxid. Med. Cell. Longev.,* 2020, 1–14.

Vidhu, V.K., Aromal, S., & Philip, D. (2011), Green synthesis of silver nanoparticles using. Macrotylomauniflorum, *SpectrochimicaActa Part A: Molecular and Biomolecular Spectroscopy,* 83, 392–397.

Waanusantigul, P., Pokrthitiyook, P., Kruatrachue, M., & Upatham, E.S. (2003). Kinetic of Basic Dye (Methylen blue) Biosorption by Giant Duck Weed (*Spirodela polyrrhiza*). *Environmental Pollution,* 125, 385-392.

Wang, M.Y., Shen, T., Wang, M., Zhang, D., & Chen J. (2013), One-pot green synthesis of Ag nanoparticles-decorated reduced graphene oxide for efficient nonenzymatic $H_2O_2$ biosensor. *Mater Lett.,* 107, 311–314. doi:10.1016/j.matlet.2013.06.031

Wang, X., Koo, J., Alexander, Y., Yang, A., Westerhof, Y., Zhang, S., Schnoor, Q., Colvin, J.L., Braam, V.L., & Alvarez, P.J. (2012). Phytostimulation of poplars and Arabidopsis exposed to silver nanoparticles and Ag+ at sublethal concentrations. *Environ. Sci. Technol.,* 47, 5442–5449.

 ISSN (online): 1595-1693

Wani, I.A., Khatoon, S., Ganguly, A., Ahmed, J., Ganguli, A.K., & Ahmed, T. (2010). Silver nanoparticles: Large scale solvothermal synthesis and optical properties. *Material Research Bellutin,* 45(8), 1033-1038

Zahoor, M., Nazir, N., Iftikhar, M., Naz, S., Zekker, I., Burlakovs, J., Uddin, F., Kamran, A.W., Kallistova, A., Pimenov, N., & Ali, K.F. (2021). A review on silver nanoparticles: Classification, various methods of synthesis, and their potential roles in biomedical applications and water treatment. *Water,* 13(16), 2216-2231.

**Citation:**
Bamigbade, A.A., Oduntan, K. D., Sulaiman, T. R., Ayeni, I., & Akiode, K. O. (2025). Dye Degradation from Aqueous Solution by Green Synthesised Silver Nanoparticles (AgNPs) from Smooth Pigweed (*Amaranthus hybridus*): Kinetics and Thermodynamics Studies. *Fountain Journal of Basic Medical and Health Sciences (FUJBMHES), 1(2), 56-76.*


ISSN (online): 1595-1693